

Cross-Study Replicability in Cluster Analysis

Lorenzo Masoero^{*}, Emma Thomas¹, Giovanni Parmigiani², Svitlana Tyekucheva², and Lorenzo Trippa²

^{*}*Email address:* lo.masoero@gmail.com

¹*Department of Biostatistics, Harvard T.H. Chan School of Public Health*

²*Department of Data Science, DFCI*

February 7, 2022

Abstract

In cancer research, clustering techniques are widely used for exploratory analyses and dimensionality reduction, playing a critical role in the identification of novel cancer subtypes, often with direct implications for patient management. As data collected by multiple research groups grows, it is increasingly feasible to investigate the replicability of clustering procedures, that is, their ability to consistently recover biologically meaningful clusters across several datasets.

In this paper, we review existing methods to assess replicability of clustering analyses, and discuss a framework for evaluating cross-study clustering replicability, useful when two or more studies are available. These approaches can be applied to any clustering algorithm and can employ different measures of similarity between partitions to quantify replicability, *globally* (i.e. for the whole sample) as well as *locally* (i.e. for individual clusters). Using experiments on synthetic and real gene expression data, we illustrate the utility of replicability metrics to evaluate if the same clusters are identified consistently across a collection of datasets.

1 Introduction

Clustering, the task of partitioning data into distinct classes, is fundamental in a variety of fields and applications. For example, in genomics, clustering procedures are used for exploratory analyses, dimensionality reduction and to identify interpretable groups within high-dimensional data, such as gene expression studies.

One of the difficulties in clustering, common to other unsupervised techniques, is the ambiguity of the notion of success. In contrast to supervised learning, where ground truth measurements can be used to validate the performance of a learning procedure (e.g., the precision of a classifier), in unsupervised learning, a

direct measure of success is not available. In applications it is however crucial to identify criteria to assess the reliability of unsupervised learning methods.

Here we consider the problem of assessing replicability of cluster analyses. We consider as a motivating example clustering in gene expression studies aiming to identify cancer subtypes. In this context, a dataset is a high dimensional collection of gene expression profiles of different patients, and cluster analyses try to identify biologically relevant groups of observations. An ideal cluster analysis identifies cancer subtypes and in turn allows scientists to develop specific and effective treatment strategies for the different subtypes.

We introduce notation and relevant background in Section 2, where we also provide a review of the existing literature. Next, in Section 3, we focus on the assessment of clustering replicability when multiple datasets are available — a question of increasing importance in biosciences, where collections of datasets generated by different research groups and institutions are often available [Hayes et al., 2006, Bernau et al., 2014, Trippa et al., 2015, of Sciences Engineering and Medicine, 2019]. We provide a guide to assess the replicability of the results of cluster analyses when multiple datasets are available. The idea underlying replicability metrics is that clusters consistently identified by independent analyses of distinct datasets can be used as a criterion to assess their replicability.

We show how to generate replicability summaries, representative of the similarity of the groups identified by a clustering method, say k -means, across independent analyses of the available datasets. Our procedure evaluates the replicability, without constraints on the choice of the clustering method, and across any number of datasets, at both a *global* scale, that is for the whole data collection, as well as at a *local* scale, that is for an individual cluster. We conclude with experimental results: we test the framework on synthetic data in Section 4, and we present an application in cancer research in Section 5. We provide code to replicate all our analysis at https://github.com/lorenzomasoero/clustering_replicability.

2 Clustering Replicability in a Single Study

With the growth of high dimensional and multi-modal datasets in several areas of science, practitioners need replicable procedures to analyze and simplify their data. In biological sciences, for example, advances in data-collection technologies allow investigators to study increasingly big datasets, with large sample sizes and feature lists (gene expression profiles, demographics, imaging). While these rich datasets come with the promise of new insights, they also present practical challenges. Analysts often need dimensionality reduction techniques to visualize and explore the data. In this context, clustering algorithms have emerged as a preeminent technique because of their scalability, ease-of-use and wide applicability. While several clustering algorithms are available, assessing the usefulness and quality of the results they produce is a difficult problem, which has received considerable interest in the literature. Here, we focus on replicability of cluster analyses.

We introduce notation in Section 2.1, and then review existing literature on replicability of cluster analyses. In our review, we group methods for replicability assessments on the basis of their underlying principles: stability-based approaches are discussed in Section 2.2, methods based on statistical tests in Section 2.3, and prediction-based approaches in Section 2.4. When possible, we distinguish between replicability metrics that assess if the result of a cluster analysis is replicable as a whole (*global*), or if an individual cluster replicates (*local*). We conclude by discussing available software for estimating clustering stability in Section 2.5.

2.1 Notation

Data A dataset $\mathbf{X} = \{x_1, \dots, x_n\}$ is a collection of datapoints, and an individual observation $x_i = [x_{i,1}, \dots, x_{i,p}]$ is a p -dimensional vector, e.g., the gene expression profile of patient i , where $x_{i,j}$ is the expression level of the j -th gene of interest.

Clustering Algorithms A clustering algorithm is a procedure \mathcal{A} which takes as input a training dataset \mathbf{X} and outputs a clustering function $\psi(\cdot; \mathcal{A}, \mathbf{X})$. The function $\psi(\cdot; \mathcal{A}, \mathbf{X})$ is a map from the input space \mathbb{R}^p to classes $\ell \in [k] := \{1, 2, \dots, k\}$:

$$\psi(\cdot; \mathcal{A}, \mathbf{X}) : \mathbb{R}^p \rightarrow [k]. \quad (1)$$

Importantly, we define $\psi(\cdot; \mathcal{A}, \mathbf{X})$ as an operator which takes as input any test point $x' \in \mathbb{R}^p$, not necessarily in \mathbf{X} , and outputs a class for this point.

Partitioning via Clustering Functions A partition of a set \mathbf{X}' is a collection of subsets U_1, \dots, U_k such that $U_j \cap U_\ell = \emptyset$ for $j \neq \ell$ and $\cup_{j=1}^k U_j = \mathbf{X}'$. Then, a clustering function such as the one defined in Equation (1) directly induces a partition of any collection of data points \mathbf{X}' . Given a training dataset \mathbf{X} and a clustering algorithm \mathcal{A} , we can partition a testing dataset \mathbf{X}' by applying the clustering function $\psi(\cdot; \mathcal{A}, \mathbf{X})$ in turn to each point $x' \in \mathbf{X}'$. Data-points sharing the same cluster label belong to the same subset of the partition, e.g. the j -th subset is given by $U_j = \{x' \in \mathbf{X}' : \psi(x'; \mathcal{A}, \mathbf{X}) = j\}$. We let $\Psi(\mathbf{X}'; \mathcal{A}, \mathbf{X}) := \{\psi(x'; \mathcal{A}, \mathbf{X}), x' \in \mathbf{X}'\}$ denote the labels of the points in the set \mathbf{X}' arising from the element-wise application of the clustering function $\psi(\cdot; \mathcal{A}, \mathbf{X})$ to $x' \in \mathbf{X}'$.

Binary Partitions For $y, x' \in \mathbb{R}^p$ and a clustering function $\psi(\cdot; \mathcal{A}, \mathbf{X})$, we define the operator $\tilde{\psi}_{x'}(\cdot; \mathcal{A}, \mathbf{X})$ to be the map which binarizes the clustering function:

$$\tilde{\psi}_{x'}(y; \mathcal{A}, \mathbf{X}) = \mathbb{1}\{\psi(y; \mathcal{A}, \mathbf{X}) = \psi(x'; \mathcal{A}, \mathbf{X})\}. \quad (2)$$

Example: k -means Let \mathcal{A} be the k -means algorithm. Given a training dataset \mathbf{X} , this algorithm works by (approximately) solving the optimization problem:

$$\min_{U_1, \dots, U_k} \sum_{\ell=1}^k \sum_{i \in U_\ell} \|x_i - c_\ell\|_2, \quad (3)$$

where the disjoint subsets U_1, \dots, U_k form a partition of \mathbf{X} . Each $c_\ell = [c_{\ell,1}, \dots, c_{\ell,p}]$ is the ℓ -th “centroid”, with components $c_{\ell,r} = (\sum_{i \in U_\ell} x_{i,r}) / |U_\ell| \in \mathbb{R}$, $r \in [p]$. We view k -means as the procedure \mathcal{A} that returns the clustering function

$$\psi(x'; \mathcal{A}, \mathbf{X}) = \arg \min_{\ell \in \{1, \dots, k\}} \|x' - c_\ell\|_2. \quad (4)$$

We write $\psi(\cdot)$ or $\psi(\cdot; \mathbf{X})$ in place of $\psi(\cdot; \mathcal{A}, \mathbf{X})$ and $\Psi(\cdot)$ or $\Psi(\cdot; \mathbf{X})$ in place of $\Psi(\cdot; \mathcal{A}, \mathbf{X})$ when \mathcal{A} and \mathbf{X} are clear from the context.

Remark: Induced Clustering Functions In many cases, the clustering function ψ is a direct output of the procedure \mathcal{A} (e.g., Equation (4) for k -means). However, there exist popular algorithms in which the direct output is just a partition of the training set (e.g., hierarchical clustering). In these cases we obtain a clustering function indirectly, via an additional classification step. A simple choice consists in adopting a nearest neighbor approach: let $z(i) \in [k]$ be the cluster label for datapoint x_i , $i = 1, \dots, n$ obtained applying \mathcal{A} to \mathbf{X} . Then, for a generic $x' \in \mathbb{R}^p$,

$$\psi(x') := z \left(\arg \min_{x_i \in \mathbf{X}} d(x', x_i) \right),$$

where $d(\cdot, \cdot)$ is a suitable distance metric on \mathbb{R}^p . We emphasize that the nearest neighbor step above could be replaced by a different classifier.

2.2 Clustering Replicability via Stability

We first review methods to evaluate the replicability of cluster analyses which rely on the notion of *stability*. The intuition underlying these methods is that a cluster analysis is replicable if the results remain similar when we repeat the same analysis several times, using the same or slightly different data.

2.2.1 Global Replicability

A first assessment of clustering replicability can be performed by analyzing the output of a clustering algorithm over multiple runs on the same dataset. A stable clustering procedure should provide the same output when the input remains the same. For example, consider again k -means: the clustering function is obtained by approximately solving the minimization in Equation (3). It is possible that,

even when repeatedly applied to the same dataset, multiple runs produce different results, because distinct initializations may identify different local minima of the objective function. Assume to run k -means twice on the same dataset \mathbf{X} , and let $\psi^{(1)}, \psi^{(2)}$ be the two learned clustering functions. Von Luxburg et al. [2010] proposed to measure replicability using the minimal matching distance, defined as the minimum number of labels switches needed to make the partitions induced by $\psi^{(1)}$ and $\psi^{(2)}$ identical:

$$d(\Psi^{(1)}(\mathbf{X}), \Psi^{(2)}(\mathbf{X})) = \min_{\pi} \sum_{i=1}^n \mathbb{1} \left[\psi^{(1)}(x_i) \neq \pi \left\{ \psi^{(2)}(x_i) \right\} \right],$$

where π is a permutation of the k labels of the clusters. We can obtain an average stability-based score of replicability by repeatedly running k -means and computing the average minimal matching distance across re-runs. See Ben-David et al. [2007] and Von Luxburg et al. [2010] for theoretical results on the stability of k -means.

A clustering algorithm could produce the same output when re-applied to the same dataset, but its output might change considerably if we just slightly change the input data. Several authors have therefore generalized the definition of stability by comparing the results of an algorithm applied to slightly different versions of the same dataset [Bryan, 2004, Lange et al., 2004, Ben-David et al., 2007]. This notion of clustering stability is widely accepted among practitioners, since a replicable clustering procedure should not be too sensitive to small perturbations of the data.

Popular approaches to produce perturbed versions of the original dataset include (i) sub sampling the data [Levine and Domany, 2001], or (ii) corrupting individual datapoints, e.g. by adding random noise [Hennig, 2007]. If the results obtained by performing clustering on the corrupted datasets are similar to the ones obtained on the original data, then the cluster analysis is stable. Instead, when the results differ across perturbed datasets — despite the fact that the datasets are similar by construction — the clustering algorithm is deemed unstable.

To illustrate, a stability-based analysis to assess the replicability of k -means on \mathbf{X} could proceed as follows. Let B be a large integer, and for every $b = 1, \dots, B$ let $\mathbf{X}^{(b)}$ be either (i) a random subsample of \mathbf{X} (e.g., a draw of $n' < n$ datapoints without replacement), (ii) a corrupted version of \mathbf{X} , in which the i -th datapoint $x_i^{(b)} = x_i + \epsilon_i^{(b)}$, where $\epsilon_i^{(b)}$ is a random error term or (iii) a combination of (i) and (ii). Then, a stability measure is obtained by averaging the minimal matching distance between the partition of \mathbf{X} learned using the full dataset, $\Psi(\mathbf{X}; \mathcal{A}, \mathbf{X})$, and the partition $\Psi(\mathbf{X}; \mathcal{A}, \mathbf{X}^{(b)})$ obtained with the b -th corrupted dataset:

$$\frac{1}{B} \sum_{b=1}^B d \left\{ \Psi(\mathbf{X}; \mathcal{A}, \mathbf{X}); \Psi(\mathbf{X}; \mathcal{A}, \mathbf{X}^{(b)}) \right\}.$$

Although here we focused on the k -means algorithm and the minimal matching distance, the description outlined above can be extended to other algorithms and discrepancy measures. For example, Fang and Wang [2012] discussed a similar

procedure which, using bootstrap replicates, aims at identifying the number of clusters present in the data. Vinh and Epps [2009] considered instead alternative metrics that replace the minimum matching distance, such as the (adjusted) Rand index and mutual information. We highlight, among other references, the thorough review by Von Luxburg et al. [2010] for additional details and examples of stability-based validation techniques tailored to cluster analyses.

2.2.2 Local Replicability

Besides assessing global replicability of a clustering algorithm, scientists might be interested in understanding the *local* replicability of a specific cluster of interest, for example because this cluster is hypothesized to be biologically relevant. One of the most influential methods for local replicability was proposed by Smolkin and Ghosh [2003]. In this work, the authors proposed the following: given a high-dimensional dataset \mathbf{X} , perform clustering on the dataset, and let U_1, \dots, U_k be the resulting clusters. Given a fraction $\alpha \in [0, 1]$ and a large integer value B , for $b = 1, \dots, B$, first select a random subset of $p' = \lfloor \alpha p \rfloor$ covariates from the p original ones. Let $\mathbf{X}^{(b)}$ be the dataset obtained by retaining for every datapoint only the $p' < p$ randomly selected covariates. Perform the same clustering procedure as before, but now on $\mathbf{X}^{(b)}$, and let $U_1^{(b)}, \dots, U_k^{(b)}$ be the resulting clusters. The stability of the j -th cluster (the j -th subset of the partition, U_j) is measured by the fraction of the B repetitions for which there exists a cluster $U_i^{(b)}$ such that $U_j \subseteq U_i^{(b)}$:

$$\frac{1}{B} \sum_{b=1}^B \mathbb{1} \left(\sum_{i=1}^k \mathbb{1}(U_j \subseteq U_i^{(b)}) > 0 \right).$$

Variations of this methods and similar ideas have also been proposed: e.g. Hennig [2007] proposed averaging the (maximum) Jaccard coefficient:

$$\frac{1}{B} \sum_{b=1}^B \max_{i=1, \dots, k} \gamma(U_j, U_i^{(b)}), \text{ with } \gamma(U_j, U_i^{(b)}) = \frac{|U_j \cap U_i^{(b)}|}{|U_j \cup U_i^{(b)}|}.$$

The mean across re-runs could be replaced by other summaries (median, quantiles).

Another notable approach for stability-based local replicability was proposed by McShane et al. [2002], specifically for genomics data. The authors propose two metrics for local clustering stability, the R -index and the D -index. Again, the method relies on considering B perturbations of the original dataset \mathbf{X} , denoted $\mathbf{X}^{(1)}, \dots, \mathbf{X}^{(B)}$, with $\mathbf{X}^{(b)} = \{x_1 + e_1^{(b)}, \dots, x_n + e_n^{(b)}\}$, where $e_i^{(b)}$ are i.i.d. mean-zero Gaussian error terms. Let U_j be again a cluster of interest in the original dataset \mathbf{X} . The R -index quantifies U_j 's stability by computing, across re-runs, the average fraction of pairs of datapoints in U_j which remains clustered together after re-clustering the perturbed dataset $\mathbf{X}^{(b)}$. Instead the D -index computes the number of “discrepancies” (additions or deletions) between the original cluster U_j and the cluster with the highest overlap in the perturbed data.

2.3 Analyses Based on Statistical Tests

Next we consider methods for the evaluation of cluster analyses where replicability is assessed via a statistical *test*, in which the null hypothesis H_0 is the absence of distinct clusters in the data. This approach shares similarities with mixture models for density estimation: the investigator evaluates if multiple components are necessary to approximate the unknown distribution of the n datapoints. Hypothesis testing can be helpful to provide evidence that \mathbf{X} includes two or more clusters by rejecting the null hypothesis of an underlying unimodal distribution.

The majority of methods in this class relies on parametric models, assuming under the null hypothesis of “no clustering structure” that the data originates from a posited parametric model. The test proceeds by comparing the value of a relevant test statistic computed using the observed data \mathbf{X} , to the distribution of the test statistic under the null hypothesis, often approximated using Monte Carlo simulations. If the value of the test statistic on the actual data \mathbf{X} is sufficiently unlikely under the null hypothesis, then H_0 is rejected. We discuss two influential hypothesis tests, proposed in McShane et al. [2002] and Liu et al. [2008]. Other approaches that involve hypothesis tests in the context of microarray data analyses include Levenstien et al. [2003], Alexe et al. [2006], Bertoni and Valentini [2007].

The test developed in McShane et al. [2002] is as follows. First, to circumvent potential pitfalls related to high dimensionality, the original training dataset $\mathbf{X} = \{x_1, \dots, x_n\}$ is projected into its principal component space and its dimensionality reduced. Only principal components projections $\tilde{\mathbf{X}} = \{\tilde{x}_1, \dots, \tilde{x}_n\}$ are retained, where \tilde{x}_i includes the first $p' \ll p$ principal components. To test the null hypothesis of no clustering structure, assume that under H_0 the datapoints are independent and Gaussian distributed. The mean $\tilde{\mu}$ and covariance matrix $\tilde{\Sigma} \in \mathbb{R}^{p' \times p'}$ are estimated using $\tilde{\mathbf{X}}$. For each (projected) datapoint $\tilde{x}_i \in \tilde{\mathbf{X}}$ the nearest neighbor distance $d_i = \min_{j \neq i} \|\tilde{x}_i - \tilde{x}_j\|^2$ is computed, as well as the CDF of these distances, $G_*(d) = n^{-1} \sum_i \mathbb{1}(d_i \leq d)$.

After generating a sequence of datasets $\tilde{\mathbf{X}}^{(b)}$, for $b = 1, \dots, B$, from the null model, the same computation is repeated for each simulated dataset to obtain the empirical CDFs $G_b(\cdot)$. Under H_0 , the CDFs $G_*(\cdot)$, $G_1(\cdot), \dots$, and $G_B(\cdot)$ are approximately identically distributed. Then, for $b \in \{\star, 1, \dots, B\}$, the following test statistics are computed:

$$s_b = \int_0^\infty \left\{ G_b(y) - \frac{1}{B} \sum_{b' \neq b} G_{b'}(y) \right\}^2 dy.$$

Each s_b can be interpreted as the distance of $G_b(\cdot)$ from $\frac{1}{B} \sum_{b' \neq b} G_{b'}(\cdot)$. The value of s_* is compared to s_1, \dots, s_B and H_0 is rejected at confidence level α if s_* is larger than the $100 \times (1 - \alpha)$ percentile of s_b , $b = 1, \dots, B$.

In Liu et al. [2008], the authors propose a statistical test in which, under the null hypothesis H_0 , datapoints x_i come from a single multivariate Gaussian

distribution. The test proposed goes as follows: first, the original dataset is partitioned into clusters using k -means. The test statistic s_0 is computed as a ratio, in which the numerator is the within-cluster sum of squared distances to the cluster mean, and the denominator is the overall sum of squared distances to the overall mean. Next, following assumptions and techniques from the literature on factor analysis, the covariance matrix of the data distribution is estimated. Under H_0 , the estimated covariance matrix is used to iteratively simulate datasets $\tilde{\mathbf{X}}^{(b)}$, for $b = 1, \dots, B$. Each datasets is again partitioned using k -means, and the corresponding test statistics s_b are computed. Also in this case, if the value of the test statistic s_0 is small with respect to s_1, \dots, s_B , then H_0 is rejected.

2.4 Cluster Analyses and Prediction Accuracy

2.4.1 Global Replicability

Last we discuss methods for the assessment of cluster analyses based on metrics of prediction accuracy, where ideas developed in the context of classification are adapted to clustering. We review two influential ones, Tibshirani and Walther [2005], Kapp and Tibshirani [2006], although other valuable contributions exist (e.g., Dudoit and Fridlyand [2002], Langfelder et al. [2011]).

Tibshirani and Walther [2005] developed a prediction-based procedure for choosing of the “optimal” number of clusters. Optimality is defined as the ability of accurately predicting clustering co-membership in a test set, based on the clustering function learned on a training set. More precisely, the authors partition the data into a training dataset \mathbf{X} and a test dataset \mathbf{X}' . Then,

- Choose k , the number of clusters, and \mathcal{A} , the clustering algorithm.
- Partition \mathbf{X} into clusters. For each $x' \in \mathbf{X}'$, let $\hat{y}(x') := \psi(x'; \mathcal{A}, \mathbf{X})$ be the cluster label assigned to datapoint x' by algorithm \mathcal{A} when trained on \mathbf{X} .
- Partition \mathbf{X}' into clusters. For every $x' \in \mathbf{X}'$ let $y(x') := \psi(x'; \mathcal{A}, \mathbf{X}')$ be the label assigned to it. Let U_1, \dots, U_k denote the subsets of the partition of \mathbf{X}' induced by $\Psi(\mathbf{X}'; \mathcal{A}, \mathbf{X}')$, and $n_j = |U_j|$, the size of subset j .
- Quantify the “prediction strength” by computing co-clustering occurrences:

$$\text{ps}(k) := \min_{1 \leq j \leq k} \left[\frac{1}{n_j(n_j - 1)} \sum_{x'_i, x'_\ell \in U_j, i \neq \ell} \mathbb{1}_{\{\hat{y}(x'_i) = \hat{y}(x'_\ell)\}} \right]. \quad (5)$$

The authors use prediction strength to identify the number of clusters k into which the dataset should be partitioned — namely, find $k = \arg \max_{k' \geq 2} \text{ps}(k')$.

2.4.2 Local Replicability

Relatedly, Kapp and Tibshirani [2006] developed a cluster-specific measure of replicability, the “in-group-proportion” [IGP]. The IGP for a given cluster U_j is the fraction of datapoints $x \in U_j$ whose nearest neighbors are also in the same group: let $\text{nn}(x_i) = \arg \min_{x' \in \mathbf{X}} d(x_i, x')$, for a distance $d(\cdot, \cdot)$,

$$\text{IGP}(U_j) = \frac{1}{|U_j|} \sum_{x \in U_j} \mathbb{1} [\text{nn}(x_i) \in U_j].$$

2.5 Available Software

There exist several packages and available software for clustering replicability. We recommend **c1Valid** [Brock et al., 2008], an *R* package for cluster analyses which implements stability based methods, as well as the **fpc** R-package [Hennig, 2015] which, among other functionalities, allows to compute the prediction strength proposed in Tibshirani and Walther [2005] and the bootstrap stability measure proposed in Fang and Wang [2012].

3 Clustering and Cross-Study Replicability

3.1 Challenges and Strategies for Cross-Study Clustering Replicability

Often, scientists interested in investigating replicability have access to *multiple* datasets, and are interested in understanding replicability properties of their analyses *across* these datasets. In this setting, more general than the one discussed in Section 2, datapoints in different datasets can be drawn from different distributions, for example because of different study designs or technical differences in the instrumentation used to measure the variables. High replicability scores within each study do not necessarily imply replicability across different datasets.

Nonetheless it is possible to make progress in this more challenging assessment by leveraging the principles underlying the prediction accuracy methods reviewed in Section 2.4. Here we provide a guide for this extension, and discuss how to leverage the ideas reviewed in Section 2 for quantifying *cross-study* clustering replicability when *multiple studies* are available, and for selecting clustering algorithms with better *cross-study* replicability summaries compared to others. Informally, we say that clustering algorithm \mathcal{A} is replicable if it is able to learn similar clustering functions across the datasets analyzed. The notion of similar clustering functions is intuitive. Consider for example two datasets \mathbf{X}, \mathbf{X}' — the “training” and “testing” dataset respectively. These could be data from independent studies probing the same molecular features on patients with similar clinical conditions. We quantify the replicability of the analyses produced by clustering algorithm \mathcal{A} by measuring the differences between the partitions of \mathbf{X}' obtained by using the clustering functions learned by training \mathcal{A} on \mathbf{X} and on

\mathbf{X}' respectively. That is, we will focus on $d(\Psi(\mathbf{X}'; \mathcal{A}, \mathbf{X}), \Psi(\mathbf{X}'; \mathcal{A}, \mathbf{X}'))$, where $d(\cdot, \cdot)$ is a measure of distance or discrepancy between two partitions of the set \mathbf{X}' . Notice that, the prediction strength already discussed in Equation (5), is a similarity metric.

We use cancer subtype validation as a motivating example: we consider multiple datasets of patients gene expressions, collected by different investigators. Replicability analysis will help us understand whether the clustering learned on the dataset collected by one investigator identifies cancer subtypes in a different dataset.

3.2 Useful Metrics for Clustering Replicability

Several measures of discrepancy between partitions have been proposed in the literature. See, e.g., Albatineh et al. [2006], Vinh et al. [2010], Jaskowiak et al. [2014]. Here we highlight two metrics which we have found useful in assessing cross-study replicability: the Rand index (RI, Rand [1971]) and the mutual information (MI), as well as their adjusted versions. In what follows, $\mathbf{U} = \{U_1, \dots, U_{k_1}\}$ and $\mathbf{V} = \{V_1, \dots, V_{k_2}\}$ denote two partitions of the set $\mathbf{X}' = \{x'_1, \dots, x'_m\}$, with $|\mathbf{U}| = k_1$ and $|\mathbf{V}| = k_2$, respectively. We briefly review them next.

The Rand Index [RI] The Rand index is a simple pair-counting discrepancy measure. It is obtained by computing the fraction of pairs of datapoints on which two different partitions \mathbf{U} and \mathbf{V} of the same set \mathbf{X} agree. Let $N_{0,0}(\mathbf{U}, \mathbf{V})$ denote the number of pairs of points which belong to different subsets in both partitions, $N_{1,1}(\mathbf{U}, \mathbf{V})$ the number of pairs which belong to the same subset in both partitions, $N_{1,0}(\mathbf{U}, \mathbf{V})$ the number of pairs which belong to the same subset in partition \mathbf{U} , but are in different subsets in partition \mathbf{V} , and symmetrically $N_{0,1}(\mathbf{U}, \mathbf{V})$ the number of pairs belonging to different subsets in partition \mathbf{U} and to the same subset in partition \mathbf{V} . Because there are exactly $\binom{m}{2}$ pairs of points, and each pair of points falls in exactly one of these categories, it follows that

$$N_{0,0}(\mathbf{U}, \mathbf{V}) + N_{0,1}(\mathbf{U}, \mathbf{V}) + N_{1,0}(\mathbf{U}, \mathbf{V}) + N_{1,1}(\mathbf{U}, \mathbf{V}) = \binom{m}{2}.$$

The Rand index for partitions \mathbf{U} , \mathbf{V} of the set \mathbf{X} is then defined as

$$\text{RI}(\mathbf{U}, \mathbf{V}) = \frac{N_{0,0}(\mathbf{U}, \mathbf{V}) + N_{1,1}(\mathbf{U}, \mathbf{V})}{\sum_{i=0}^1 \sum_{j=0}^1 N_{i,j}(\mathbf{U}, \mathbf{V})} = \frac{N_{0,0}(\mathbf{U}, \mathbf{V}) + N_{1,1}(\mathbf{U}, \mathbf{V})}{\binom{n}{2}}. \quad (6)$$

Given datasets \mathbf{X} and \mathbf{X}' , and the clustering functions $\psi(\cdot; \mathbf{X})$ and $\psi(\cdot; \mathbf{X}')$, let \mathbf{U} and \mathbf{V} be the partitions of \mathbf{X}' induced by the cluster labels $\Psi(\mathbf{X}'; \mathbf{X})$ and $\Psi(\mathbf{X}'; \mathbf{X}')$ respectively. We use the Rand index as a replicability measure of the clustering learned on \mathbf{X} and tested on \mathbf{X}' .

The Mutual Information [MI] The mutual information is an information theoretic quantity which provides a measure of the dependence between two random variables: it is always nonnegative, and achieves 0 when the random variables are independent. Moreover, it is bounded above by the entropy of the two random variables, achieved when one of the two random variables can be expressed as a deterministic function of the other. In clustering, the mutual information between two partitions quantifies how much information about one cluster membership is revealed by knowing the other. Given two partitions \mathbf{U}, \mathbf{V} of \mathbf{X}' , their mutual information is

$$\text{MI}(\mathbf{U}, \mathbf{V}) = \sum_{i=1}^{k_1} \sum_{j=1}^{k_2} \frac{|U_i \cap V_j|}{m} \log \left(\frac{|U_i \cap V_j|/m}{|U_i| \times |V_j|/m^2} \right). \quad (7)$$

Given datasets \mathbf{X} and \mathbf{X}' and clustering functions $\psi(\cdot; \mathbf{X})$ and $\psi(\cdot; \mathbf{X}')$, let \mathbf{U}, \mathbf{V} be the partitions of \mathbf{X}' induced by cluster labels $\Psi(\mathbf{X}'; \mathbf{X})$ and $\Psi(\mathbf{X}'; \mathbf{X}')$ respectively. We use the MI as a replicability measure of the cluster analyses.

Adjustments to Improve Interpretability A desirable property that should be shared across replicability measures is that they should yield, at least in expectation, a constant and common baseline value when applied to independent random partitions. That is to say, if we repeatedly create independent random partitions \mathbf{U} and \mathbf{V} of \mathbf{X}' , then on average the replicability measure should be a baseline, constant value. This is not the case for either the Rand index or the mutual information. General solutions to derive an index which satisfies this property when applied to independent random clusterings were proposed in Hubert and Arabie [1985]. First, we fix a probabilistic model according to which random partitions are generated. We follow the standard convention and choose the permutation model [Lancaster and Seneta, 1969], in which clusterings are generated at random under the constraint of a fixed number of clusters, and a fixed number of points within each cluster. Under this model, we define the following adjusted metric:

$$r^*(\mathbf{U}, \mathbf{V}) = \frac{r(\mathbf{U}, \mathbf{V}) - \mathbb{E}_{\tilde{\mathbf{U}}, \tilde{\mathbf{V}}}[r(\tilde{\mathbf{U}}, \tilde{\mathbf{V}})]}{\max_{\mathbf{U}', \mathbf{V}'}\{r(\mathbf{U}', \mathbf{V}')\} - \mathbb{E}_{\tilde{\mathbf{U}}, \tilde{\mathbf{V}}}[r(\tilde{\mathbf{U}}, \tilde{\mathbf{V}})]},$$

where $r(\mathbf{U}, \mathbf{V})$ denotes the unadjusted replicability metric (RI or MI) between partitions \mathbf{U} and \mathbf{V} of the same dataset \mathbf{X} . Given \mathbf{U} and \mathbf{V} and their subsets' sizes, the terms $\mathbb{E}_{\tilde{\mathbf{U}}, \tilde{\mathbf{V}}}[r(\tilde{\mathbf{U}}, \tilde{\mathbf{V}})]$ and $\max_{\mathbf{U}', \mathbf{V}'}\{\mathbf{U}', \mathbf{V}'\}$ appearing in the denominator of the equation above are obtained by respectively integrating and maximizing over the set of partitions with k_1 and k_2 subsets having sizes $\{|U_k|\}_{k=1}^{k_1}$ and $\{|V_j|\}_{j=1}^{k_2}$ with respect to the permutation model of Lancaster and Seneta [1969]. We henceforth adopt the adjusted replicability indices described above: the adjusted Rand index (ARI) and mutual information (AMI), and replace them in Equations (6) and (7). For additional details, see Vinh et al. [2009, 2010].

3.3 Quantifying Cross-Study Replicability of Cluster Analyses

3.3.1 Replicability on a Single Testing Dataset

Let \mathbf{X}, \mathbf{X}' be independent datasets consisting of n and m data points respectively. To capture heterogeneity owing to different measurement technologies, errors in the measurement processes, and other factors, we model each dataset as a collection of independent and identically distributed draws from separate distribution F_1 and F_2 with support on \mathbb{R}^p . Our goal is to evaluate the replicability of clustering algorithm \mathcal{A} trained on data \mathbf{X} drawn from F_1 and validated on data \mathbf{X}' from F_2 . To measure this, we define the cross-study cluster analysis replicability index

$$R(\mathbf{X}'; \mathcal{A}, \mathbf{X}) = \mathbb{E}[r^*(\Psi(\mathbf{Z}'; \mathcal{A}, \mathbf{Z}), \Psi(\mathbf{Z}'; \mathcal{A}, \mathbf{Z}'))], \quad (8)$$

where $\mathbf{Z} = \{Z_1, \dots, Z_n\}$ is a collection of n i.i.d. random replicates from F_1 , and $\mathbf{Z}' = \{Z'_1, \dots, Z'_m\}$ is a collection of m i.i.d. random replicates from F_2 . We refer to the index defined by Equation (8) as R . A point estimate of R is readily available by computing $\hat{R}(\mathbf{X}; \mathcal{A}, \mathbf{X}') = r^*(\Psi(\mathbf{X}'; \mathcal{A}, \mathbf{X}), \Psi(\mathbf{X}'; \mathcal{A}, \mathbf{X}'))$. To produce interval estimates of R , we suggest a bootstrap approach, similar to those proposed for within-study performance of clustering (see Fang and Wang [2012] for related applications of resampling methods). We fix a number B_1 of bootstrap replicates and for each $b \in [B_1]$, we generate bootstrap datasets $\mathbf{X}^{(b)}, \mathbf{X}'^{(b)}$ by sampling with replacement n and m data points from \mathbf{X} and \mathbf{X}' respectively. For every $b \in [B_1]$, we estimate the replicability score $\hat{R}^{(b)} := r^*(\Psi(\mathbf{X}'^{(b)}; \mathcal{A}, \mathbf{X}^{(b)}), \Psi(\mathbf{X}'^{(b)}; \mathcal{A}, \mathbf{X}'^{(b)}))$. We use the values $\{\hat{R}^{(1)}, \dots, \hat{R}^{(B_1)}\}$ to estimate the variability of \hat{R} . We summarize our procedure in Algorithm 1.

3.3.2 Replicability Across a Collection of Datasets

We now extend the analysis of Section 3.3.1 to the scenario in which a collection of $S > 2$ datasets are available. Let $\mathcal{X} = \{\mathbf{X}_1, \dots, \mathbf{X}_S\}$ be a collection of datasets, each \mathbf{X}_s containing n_s observations of the same p features. Using the procedure of Section 3.3.1 we compute pairwise replicability scores, $r^*(\Psi(\mathbf{X}_t; \mathcal{A}, \mathbf{X}_s), \Psi(\mathbf{X}_t; \mathcal{A}, \mathbf{X}_s))$ for all $s \neq t$. We obtain the cross-study replicability of algorithm \mathcal{A} trained on dataset \mathbf{X}_1 and tested on $\mathbf{X}_{s'}, s' = 2, \dots, S$ by averaging over the corresponding scores:

$$\mathcal{R}(\{\mathbf{X}_{s'}\}_{s'=2,\dots,S}; \mathcal{A}, \mathbf{X}_1) = \frac{1}{S-1} \sum_{s' \neq 1} R(\mathbf{X}_{s'}; \mathcal{A}, \mathbf{X}_1), \quad (9)$$

with $R(\mathbf{X}_{s'}; \mathcal{A}, \mathbf{X}_s)$ defined in Equation (8). Similar expressions can be defined for training sets other than \mathbf{X}_1 . A point estimate of $\mathcal{R} := \mathcal{R}(\{\mathbf{X}_{s'}\}_{s'=2,\dots,S}; \mathcal{A}, \mathbf{X}_1)$ is obtained by replacing each score $R(\mathbf{X}_{s'}; \mathcal{A}, \mathbf{X}_1)$ with its sample counterpart $\hat{R}(\mathbf{X}_{s'}; \mathcal{A}, \mathbf{X}_1)$. The same approach as before is used to produce interval estimates of \mathcal{R} . Fix a number B_2 of iterations, and for each $b \in [B_2]$

draw a bootstrap copy $\mathbf{X}_s^{(b)}$ from \mathbf{X}_s , $s \in [S]$. We learn clustering functions $\psi(\cdot; \mathcal{A}, \mathbf{X}_s^{(b)})$, $s \in [S]$, and compute for each $s' = 2, \dots, S$ the replicability index $\hat{R}_{s'}^{(b)} := r^*(\Psi(\mathbf{X}_{s'}^{(b)}; \mathcal{A}, \mathbf{X}_1^{(b)}), \Psi(\mathbf{X}_{s'}^{(b)}; \mathcal{A}, \mathbf{X}_{s'}^{(b)}))$. Then, for every $b \in [B_2]$, compute $\hat{\mathcal{R}}^{(b)} := (\hat{R}_2^{(b)} + \dots + \hat{R}_S^{(b)})/(S-1)$. The values $\{\hat{\mathcal{R}}_1^{(1)}, \dots, \hat{\mathcal{R}}_1^{(B_2)}\}$ are used to estimate confidence intervals around $\hat{\mathcal{R}}(\{\mathbf{X}_{s'}\}_{s'=2,\dots,S}; \mathcal{A}, \mathbf{X}_1)$, as described in Algorithm 2.

```

1: procedure ALGORITHM 1
2:   Fix clustering algorithm  $\mathcal{A}$ , replicability index  $r$ , number of bootstrap
   iterations  $B_1$ . Let  $\mathbf{X}$  and  $\mathbf{X}'$  be training and testing datasets.
3:   for  $b \in 1, \dots, B_1$  do
4:     Draw bootstrap samples  $\mathbf{X}^{(b)}, \mathbf{X}'^{(b)}$  from  $\mathbf{X}, \mathbf{X}'$  respectively.
5:     Learn  $\psi(\cdot; \mathbf{X}^{(b)})$  and  $\psi(\cdot; \mathbf{X}'^{(b)})$ .
6:     Compute  $\hat{R}^{(b)} = r^*(\Psi(\mathbf{X}'^{(b)}; \mathbf{X}^{(b)}), \Psi(\mathbf{X}'^{(b)}; \mathbf{X}^{(b)}))$ .
7:   return  $\hat{R}^{(1)}, \dots, \hat{R}^{(B_1)}$ .
8: procedure ALGORITHM 2
9:   Fix clustering algorithm  $\mathcal{A}$ , replicability index  $r$ , number of bootstrap
   iterations  $B_2$ , training dataset  $\mathbf{X}_t$ ,  $t \in [S]$ . Let  $\mathcal{X} = \{X_1, \dots, X_S\}$  be the
   collection of available datasets.
10:  for  $b = 1, \dots, B_2$  do
11:    for  $s = 1, \dots, S$  do
12:      Draw bootstrap sample  $\mathbf{X}_s^{(b)}$  from  $\mathbf{X}_s$ . Learn  $\psi(\cdot; \mathbf{X}_s^{(b)})$ .
13:      for  $s' = 1, \dots, S$ ,  $s' \neq t$  do
14:        Compute  $\hat{R}_{s'}^{(b)} = r^*(\Psi(\mathbf{X}_{s'}^{(b)}; \mathbf{X}_t^{(b)}), \Psi(\mathbf{X}_{s'}^{(b)}; \mathbf{X}_{s'}^{(b)}))$ .
15:      Compute  $\hat{\mathcal{R}}^{(b)} = \frac{1}{S-1} \sum_{s' \neq t} \hat{R}_{s'}^{(b)}$ .
16:    return  $\hat{\mathcal{R}}^{(1)}, \dots, \hat{\mathcal{R}}^{(B_2)}$ .

```

3.3.3 Local Replicability: Validating Individual Clusters

The replicability indices of Sections 3.3.1 and 3.3.2 provide measures to quantify which clustering procedures are reproducible across multiple datasets at a *global* scale. A natural additional desideratum for a reproducible clustering procedure is that the partitions it will induce should be similar locally as well.

Sometimes, the clusterings found on two or more datasets agree on the majority of the sample space, but disagree on a smaller portion. For example, when two datasets are available, one clustering might completely miss one group that is clearly identified by the other. The replicability scores provided by Algorithm 1 and 2 can fail to capture this pattern. Conversely, it may be that the two clusterings disagree almost everywhere, but are able to identify one or a few robust clusters. In this case, the replicability scores might be poor, and fail to provide insight about which clusters are reproduced across datasets. In applications, measuring which clusters replicate across datasets is important, as it can provide insights about the presence or absence of specific groups of

practical interest. Discrepancies can arise from a variety of factors, including different study designs.

As before, let \mathbf{X} and \mathbf{X}' be the training and testing datasets, from distributions F_1 and F_2 respectively. We now present a strategy to leverage the replicability scores when one is interested in understanding local replicability, with respect to a point of interest $x \in \mathbb{R}^p$, for example x can be a specific patient clinical profile. We can quantify whether clustering algorithm \mathcal{A} produces similar results in the neighborhood of x when trained on data \mathbf{X} and tested on data \mathbf{X}' via the following “local replicability score” (LR):

$$\text{LR}(\mathbf{X}'; \mathcal{A}, \mathbf{X}, x) = \mathbb{E}[r^*(\tilde{\Psi}_x(\mathbf{Z}'; \mathcal{A}, \mathbf{Z}), \tilde{\Psi}_x(\mathbf{Z}'; \mathcal{A}, \mathbf{Z}'))]. \quad (10)$$

Notice that the local replicability score LR is simply obtained by replacing the clustering function ψ used in Equation (8) with the binary clustering operator $\tilde{\psi}_x$ of Equation (2). If x belongs to a reproducible cluster, then the two binary partitions should be similar, and the local replicability score high. Conversely, if x is a data point within a cluster with low reproducibility, these binary partitions differ, and local replicability scores will be low. We adopt the same approach used in Algorithm 1 and 2 to obtain bootstrap confidence intervals (see Algorithm 3).

Cluster-Specific Replicability The procedure outlined above quantifies replicability with respect to a single point, but the same strategy can be used to assess replicability at a cluster level. For example, to assess the replicability of cluster $U_1 \subset \mathbf{X}$, we average the local replicability scores with respect to all points $x \in U_1$.

Multiple Studies When multiple studies $\mathbf{X}_1, \dots, \mathbf{X}_S$ are available and we are interested in studying the local replicability of a clustering learned on a training set \mathbf{X}_s when validated against \mathbf{X}_t , $t \neq s$, we can simply perform Algorithm 3 for all couples of datasets (s, t) , $t = 1, \dots, s-1, s+1, \dots, S$.

Algorithm 3

```

1: procedure ALGORITHM 3
2:   Fix clustering algorithm, replicability index  $r$ , number of bootstrap
   iterations  $B_3$ ,  $x \in \mathbb{R}^p$ .
3:   for  $b = 1, \dots, B_3$  do
4:     Draw bootstrap samples  $\mathbf{X}^{(b)}$  from  $\mathbf{X}$ , and  $\mathbf{X}'^{(b)}$  from  $\mathbf{X}'$ .
5:     Learn  $\psi(\cdot; \mathbf{X}^{(b)})$  and  $\psi(\cdot; \mathbf{X}'^{(b)})$ .
6:     Compute  $\widehat{\text{LR}}^{(b)} := r^*(\tilde{\Psi}_x(\mathbf{X}'^{(b)}; \mathbf{X}^{(b)}), \tilde{\Psi}_x(\mathbf{X}'^{(b)}; \mathbf{X}^{(b)}))$ 
7:   return  $\widehat{\text{LR}}^{(1)}, \dots, \widehat{\text{LR}}^{(B_3)}$ 

```

4 Simulation Study

4.1 Homogeneous Datasets

Let \mathbf{X}, \mathbf{X}' be training and testing datasets with n and m datapoints respectively from the same distribution F — an assumption later relaxed. Here, we consider properties of the replicability index when used for choosing the number of clusters. We consider four popular clustering algorithms: Birch [Zhang et al., 1996], k -means, mini-batch k -means [Lloyd, 1982], and agglomerative clustering [Ward Jr, 1963]. All these procedures take the number of clusters k as an input. We expect replicability scores to be high when an appropriate number of clusters is chosen.

We use a collection of benchmark datasets (see the first column of Figure 1) [Fränti and Sieranoja, 2018]. We partition each dataset into training and testing sets of equal size, let $\text{range}_{40} = \{2, 3, \dots, 40\}$ and run Algorithm 1 for each clustering algorithm for $B_1 = 100$ bootstrap iterations. The results are illustrated in Figure 1. We highlight three features of the cross-study replicability estimates:

- When the clusters are well separated, and the clustering algorithms used are appropriate for the shape of the clusters, the replicability indices achieve the highest scores at the “true” number of clusters (e.g. datasets A and B).
- When the number of clusters is less obvious, as in dataset C , the replicability scores tend to be less peaked around a single value, indicating uncertainty on the number of clusters that should be selected to maximize replicability.
- Sometimes, a clustering structure is present in the data, but algorithms fail to capture it. For example, for dataset D , the only successful algorithm is DBSCAN (Ester et al. [1996], purple line), which achieves good replicability scores for $k = 2, 3$. In this case (D), the replicability index can aid the choice of the most appropriate clustering algorithm for the data at hand.

4.2 Heterogeneous Datasets

To test Algorithm 2, we consider datasets drawn from a Gaussian mixture models which incorporates heterogeneity of the data generating distribution, and clustering of studies. For $s \in [S]$, let z_s let be the index identifying the distribution from which dataset s is generated, and $\pi_\ell^{(z_s)} \in (0, 1)$ for every $\ell \in [k]$, $\sum_\ell \pi_\ell^{(z_s)} = 1$ be mixing proportions. The data generating model is:

$$x_{s,i} \stackrel{i.i.d.}{\sim} F_{z_s} = \sum_{\ell=1}^k \pi_\ell^{(z_s)} \mathcal{N} \left(\mu_\ell^{(z_s)}, \Sigma_\ell^{(z_s)} \right) \quad \text{for } s = 1, \dots, S \text{ and } i = 1, \dots, n_s,$$

where $\mathcal{N}(\mu_\ell^{(z_s)}, \Sigma_\ell^{(z_s)})$ denotes a Gaussian distribution with mean $\mu_\ell^{(z_s)}$ and covariance matrix $\Sigma_\ell^{(z_s)}$. We set $S = 4$ and assume $\mathbf{X}_1, \mathbf{X}_2$ are drawn from the same mixture of Gaussians F_1 (i.e. $z_1 = z_2 = 1$), while $\mathbf{X}_3, \mathbf{X}_4$ are drawn from

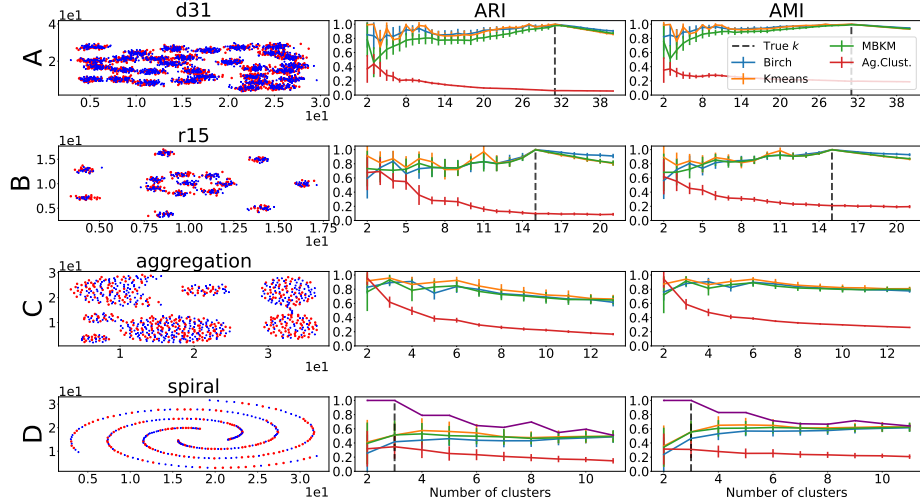


Figure 1: Reproducibility scores produced by Algorithm 1 on benchmark datasets [Fränti and Sieranoja, 2018]. Left column: datasets (*d31* (A), *r15* (B), *aggregation* (C), *spiral* (D)) randomly divided in training (red points) and testing (blue points) datasets of equal size. Center and right columns: replicability scores (vertical axis) using AMI (center) and ARI (right), versus number of clusters k (horizontal axis). We used Algorithm 1 with $B = 100$ bootstrap iterations across different input values for the. We plot the mean score \pm one standard deviation across bootstrap runs. The number of data points in datasets *A* – *D* varies widely (*d31*: $n = 3100$, *r15*: $n = 600$, *aggregation*: $n = 788$, *spiral*: $n = 312$).

a second, different mixture of Gaussians F_2 (i.e. $z_3 = z_4 = 2$). Specifically, F_1 and F_2 are defined as follows: for $k = 16$, $z \in \{1, 2\}$, and $\Sigma_\ell^{(z)} = \sigma I$, where I is the identity matrix and $\sigma = 1$ is a scaling parameter. The mean vectors $\mu_\ell^{(1)} \in \mathbb{R}^{64}, \ell \in [16]$ of F_1 induce well separated components.

The mean vectors $\mu_\ell^{(2)} \in \mathbb{R}^{64}, \ell \in [16]$ of F_2 are obtained as follows: first a permutation of the first 32 coordinates $g(\cdot)$ is chosen, and then each vector $\mu_\ell^{(2)}$ is obtained by permuting the first 32 coordinates of $\mu_\ell^{(2)}$ according to $g(\cdot)$. In this way, both F_1 and F_2 have $k = 16$ well separated - albeit, different - components (see [Fränti et al., 2006] for further description of these distributions).

We compute and report, for every pair \mathbf{X}_s and \mathbf{X}_t of datasets, the average replicability score (Figure 2) for different clustering methods. As expected, replicability scores are always higher when comparing two datasets coming from the same distribution, hence sharing the same clustering structure (top left and bottom right block diagonals of panels in Figure 2), while they are substantially lower when comparing datasets from different distributions. We also notice that all the clustering algorithms have better replicability when the correct number of

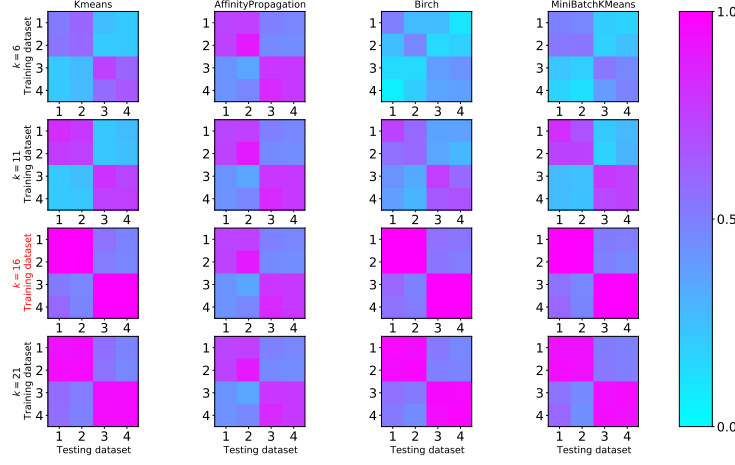


Figure 2: Average replicability scores (ARI) for 4 datasets in \mathbb{R}^{64} ($B = 100$ bootstrap runs) across different numbers of clusters k (rows: $k \in \{6, 11, 16, 21\}$, 16 is the true number of clusters) and algorithms (columns: k -means, Affinity propagation, Birch and Mini Batch k -means).

clusters is specified as an input, and that *Affinity propagation* [Frey and Dueck, 2007] seems to be performing overall worse than the other algorithms.

4.3 Local Replicability

To illustrate Algorithm 3, we consider $S = 2$ datasets, \mathbf{X}, \mathbf{X}' with 100 datapoints each, drawn from Gaussian mixture models F_1, F_2 with three components and support on \mathbb{R}^2 (Figure 3). F_1, F_2 share two of the three components:

$$F_1 = \sum_{j \in \{A, B, C\}} \frac{1}{3} \mathcal{N}(\mu_j, \sigma I), \quad \text{and} \quad F_2 = \sum_{\ell \in \{A, B, D\}} \frac{1}{3} \mathcal{N}(\mu_\ell, \sigma I). \quad (11)$$

We let $\sigma = 0.2$, $\mu_A = [-2, -2]^\top$, $\mu_B = [0, 2]^\top$, $\mu_C = [2, -2]^\top$ and $\mu_D = [-13/10, 13/20]^\top$. We refer to the mixture component identified by μ_A as component A , and similarly for the other components B, C, D . \mathbf{X} has three well separated clusters, while two of the three clusters in \mathbf{X}' are closer to each other. The goal here is to quantify, at a fixed data point x , local replicability, as discussed in Section 3.3.3. For example, x could be a point of \mathbf{X}, \mathbf{X}' , or any point in the support of the distribution. In our experiments, Algorithm 3 is able to capture the different replicability properties of individual clusters, providing substantially different scores for points belonging to different clusters. We illustrate the mechanics of the algorithm, and its ability to capture local replicability in Figure 4. In column (a) of Figure 4, we consider a point x_A close to μ_A , which does not belong to the \mathbf{X} and \mathbf{X}' datasets, and is identified by the ∇ symbol. Component A is present both in \mathbf{X} and \mathbf{X}' , and the associated

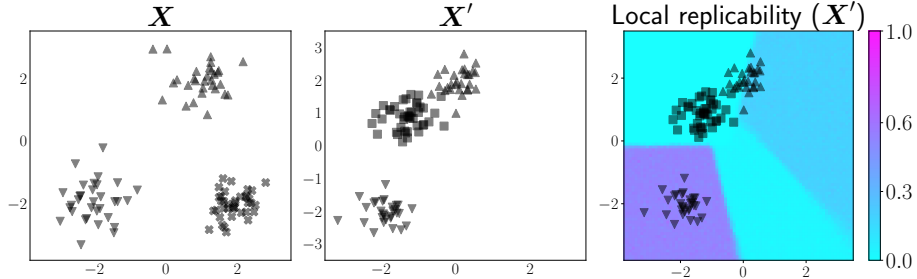


Figure 3: Local replicability. Left: training dataset \mathbf{X} (from F_1). Center: testing dataset \mathbf{X}' (from F_2 , Equation (11)). Different markers identify different components: $\nabla : A, \Delta : B, \times : C, \square : D$. Right: local replicability on \mathbf{X}' : we plot points in \mathbf{X}' , and color the sample space according to the local replicability scores of the partition learned on \mathbf{X} when tested on \mathbf{X}' . Scores (ARI) are obtained by averaging $B_3 = 100$ bootstrap runs over a grid of 250×250 equally spaced points.

cluster replicates across the two datasets. Indeed, across the $B_3 = 100$ iterations, the two binary partitions $\tilde{\Psi}_{x_A}(\mathbf{X}'^{(b)}, \mathbf{X}^{(b)})$ and $\tilde{\Psi}_{x_A}(\mathbf{X}'^{(b)}, \mathbf{X}'^{(b)})$ (top, bottom row) are similar. In column (b), we consider instead a point x_B belonging to the cluster induced by component B , identified by the Δ symbol. In \mathbf{X} , this cluster is well separated from the clusters induced by the other components. However, in \mathbf{X}' , the cluster induced by component B is close to the cluster induced by the component D , whose data points are identified with the \square symbol. The replicability score associated with x_B captures this: the binary partitions $\tilde{\Psi}_{x_B}(\mathbf{X}; \mathbf{X})$ and $\tilde{\Psi}_{x_B}(\mathbf{X}'; \mathbf{X}')$ are different. Indeed, $\tilde{\Psi}_{x_B}(\mathbf{X}'; \mathbf{X})$ incorrectly indicates points from the components B and D as belonging to the same cluster, while the partition $\tilde{\Psi}_{x_B}(\mathbf{X}'; \mathbf{X}')$ does not incur into this problem. This discrepancy negatively affects the local replicability score. Last, in column (c), we consider a point x_C that belongs to the cluster component C in \mathbf{X} (\times symbol). In this case, the scores are essentially equal to 0, since this cluster is absent in \mathbf{X}' .

5 Breast Cancer Gene Expression Datasets

In this section, we illustrate the application of clustering replicability metrics in publicly available breast cancer gene expression datasets. One of the important scientific goals of the original studies was the identification of tumor subtypes. We consider the Mainz [Schroeder et al., 2011a], Transbig [Schroeder et al., 2011b] and Vdx [Schroeder et al., 2011c] datasets. These datasets have been processed and come in the form of a matrix, $\mathbf{X} \in \mathbb{R}^{n \times p}$, where n is the number of samples and p is the number of gene expression measurements. We work with the $p = 22,283$ genes shared by all datasets. The sample sizes vary (Mainz,

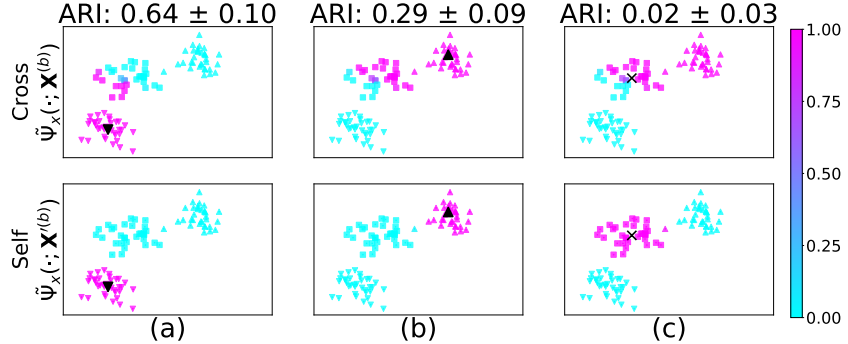


Figure 4: Local replicability. Both rows show the test dataset \mathbf{X}' . Column (a): we fix a test point x_A from component A (in black). We color each data point $x' \in \mathbf{X}'$ according to the average of $\{\tilde{\psi}_{x_A}(x'; \mathbf{X}^{(b)})\}_{b=1}^{1000}$ (top row), $\{\tilde{\psi}_{x_A}(x'; \mathbf{X}'^{(b)})\}_{b=1}^{1000}$ (bottom row). $\mathbf{X}^{(b)}, \mathbf{X}'^{(b)}$ are bootstrap draws from \mathbf{X}, \mathbf{X}' . We compute the LR (ARI) $\{r^*(\tilde{\Psi}_{x_A}(\mathbf{X}^{(b)}; \mathbf{X}^{(b)}), \tilde{\Psi}_{x_A}(\mathbf{X}'^{(b)}; \mathbf{X}'^{(b)}))\}_{b=1}^{1000}$, and report the average score \pm one standard deviation on top of column (a). This is high whenever the color pattern in the two rows is similar. Columns (b) and (c) replicate the analysis using points x_B, x_C from components B, C respectively. We use k -means, with $k = 3$.

$n_s = 200$, Transbig, $n_s = 198$, Vdx, $n_s = 344$.

Breast tumors can be classified into subtypes characterized by distinct molecular markers and clinical characteristics. There are four established molecular subtypes of breast cancer. Luminal A tumors are less aggressive than the other subtypes, have lower proliferation, express hormone receptors Estrogen Receptor (ER) and Progesteron Receptor (PR) and do not express the ERBB2 gene. These tumors are sensitive to endocrine therapy and have better prognosis compared to the other subtypes. Luminal B tumors are ER and PR positive, have higher proliferation and may or may not have ERBB2 expression. These tumors are less responsive to hormonal therapy and are more aggressive. The Her2+ subtype is characterized by increased expression of ERBB2 and low levels of ER and PR expression. This tumor subtype is aggressive and patients do not respond to endocrine therapy. Treatment options include ERBB2-targeted therapies. Basal-like (or triple negative) breast cancer subtype is characterized by low levels of ER, PR and ERBB2 expression. This is the most aggressive subtype with first and later therapy lines often limited to single-agent chemotherapy [Waks and Winer, 2019]. These subtypes were first identified by applying unsupervised hierarchical clustering to gene expression data from breast tumor tissues [Perou et al., 2000].

In our experiments, for the purpose of comparisons, we take advantage of previously proposed subsets of genes: the PAM50 subset [Parker et al., 2009], which contains fifty genes, and the three genes [3G] subset proposed by Haibe-

Kains et al. [2012].

5.1 Global replicability scores

First, we compare the replicability scores of simple clustering methods using Algorithm 1 on the three datasets considered. We use in turn each pair of datasets as training and testing, and analyze how the replicability properties change as we vary (i) the replicability metric, (ii) the training/testing pair, (iii) the clustering algorithm and the number of clusters k , and (iv) the genes subsets (Figure 5). Four observations emerge: (i) the relative ranking of clustering methods with respect to replicability scores is robust to the choice of ARI or AMI, and (ii) replicability scores are generally comparable across most pairs of training and testing datasets and produce similar results when the roles of \mathbf{X} and \mathbf{X}' are reversed. (iii) The choices of clustering algorithm and k plays instead a much bigger role in determining replicability scores. Birch and k -means tend to achieve higher replicability, while agglomerative clustering generally yields lower scores. To investigate replicability across different values of the number of clusters k , in a similar fashion to what was done in Section 4, we compute replicability scores for $k \in \{2, 3, \dots, 8\}$. The genes used impact our findings (iv): when using the 3G subset, $k = 3$ yields the highest replicability scores, while with the PAM 50 subset, especially with k -means, $k = 4$ achieves the highest scores.

The replicability metric provided consistent results with the subtypes published in Parker et al. [2009] and Haibe-Kains et al. [2012]. Namely, clustering functions that achieve high replicability scores produce partitions that are similar to the classification-based subtypes. This provides evidence that reproducible partitions are also consistent with well accepted biological findings.

5.2 Local replicability scores

Last, we illustrate a local replicability analysis. We test Algorithm 3 on the three datasets considered, using both the 3G and PAM50 gene subsets. We find that the cluster associated with the Basal subtype is the easiest to identify and the most robust, with the highest local replicability score. Luminal A and Luminal B are harder to distinguish, and are associated with lower local replicability scores.

In Figure 6 we provide a visualization of our findings. We use the 3G subset, the Transbig (\mathbf{X}') dataset [Schroeder et al., 2011b] for testing, and the Mainz (\mathbf{X}) dataset [Schroeder et al., 2011a] for training. To produce Figure 6, for each point $x \in \mathbf{X}'$ we compute the local replicability score using Algorithm 3, using k -means with $k = 4$, \mathbf{X} as training set and $B = 100$ bootstrap iterations. To group datapoints in \mathbf{X}' into different clusters, we use $\Psi(\mathbf{X}'; \mathbf{X})$. The partition obtained closely resembles the model-based signature $\Pi_{3G}(\mathbf{X}')$ provided by Haibe-Kains et al. [2012]. We therefore match each learned cluster to one of the cancer subtypes labels, so that each cluster corresponded to one cancer subtype (Luminal A, Luminal B, Basal, Her2+). The average local replicability scores within each

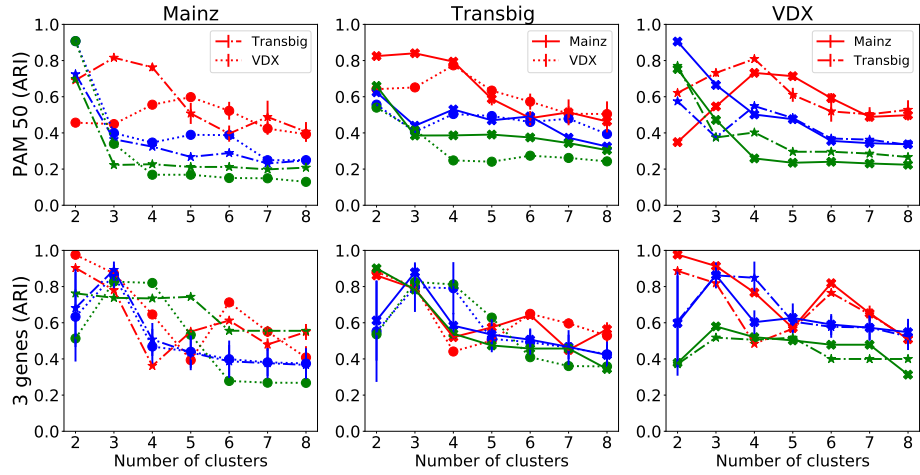


Figure 5: Average replicability scores using Algorithm 1 on Schroeder et al. [2011a,b,c] datasets. Rows identify gene subsets (top: PAM50 [Parker et al., 2009], bottom: 3G [Haibe-Kains et al., 2012]), columns identify testing datasets (left, center, right: Schroeder et al. [2011a,b,c]). For each test data/gene subset pair, we separately use each of the remaining two datasets as the training set. Line styles identify the training set used. We use k -means (red), Birch (green), and agglomerative clustering (blue), for $k \in \{2, 3, \dots, 8\}$, and report the average replicability scores (ARI) across $B = 100$ iterations \pm one standard deviation (vertical axis).

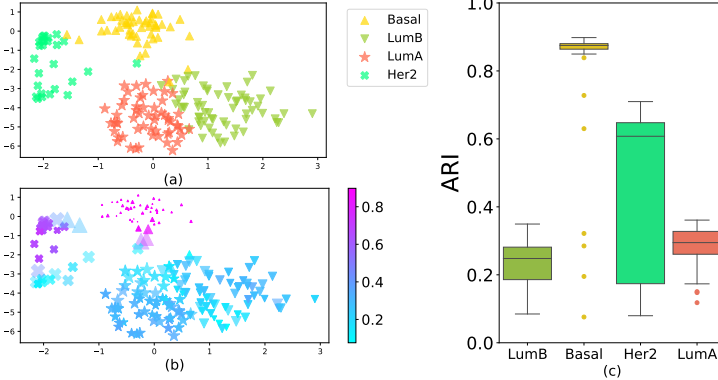


Figure 6: Local replicability of observed points in Transbig (\mathbf{X}' , Schroeder et al. [2011b]) when Mainz (\mathbf{X} , Schroeder et al. [2011a]) is used for training. We use the 3G subset [Haibe-Kains et al., 2012] and k -means, $k = 4$. In (a), we visualize \mathbf{X}' . Points are grouped into different clusters according to $\Psi(\mathbf{X}'; \mathbf{X})$, which closely resembles $\Pi_{3G}(\mathbf{X}')$, so we can assign one cancer subtype to each cluster. In (b), we report the local replicability scores obtained by running Algorithm 3 on every point $x' \in \mathbf{X}'$. Colors reflects the average local replicability (AMI) score, while the size and transparency are proportional to the standard deviation across the bootstrap iterations: larger points have more variable scores. We plot the data using a tSNE embedding with well separated clusters [Maaten and Hinton, 2008]. In (c), for each cluster subtype (as defined by $\Psi(\mathbf{X}'; \mathbf{X})$), we report ARI scores.

block of the partition confirm what expected: the Basal subtype is the most reproducible, while Luminal A and Luminal B are the least reproducible.

6 Discussion

In this paper, we provided a cohesive review of existing methods for replicability of clustering analyses, and applied validation metrics within a framework to assess replicability of clustering when multiple datasets are available. This approach allows to quantify replicability with any number of datasets and using any clustering algorithm, at a local, as well as at a global scale.

We find in experiments that the replicability scores obtained can guide practitioners in choosing appropriate clustering algorithms and tuning relevant parameters, such as the number of clusters used in the analysis. While we discussed and applied our method to gene expression data for cancer sub-typing, the methodology is general, and can be applied to different collections of datasets.

Our evaluation procedures build on the bootstrap method. In principle, replicability scores could be obtained by comparing study-specific clustering results, avoiding bootstrapping. However, in our analyses, we find that using bootstrap

subsamples for computing uncertainty summaries and interval estimates, makes the replicability scores more informative. Moreover, the bootstrap approach mitigates the impact of outliers on the replicability scores and reduces the risk of negatively biased scores due to convergence to a spurious local optimum of iterative clustering procedures such as k -means.

There are several directions in which the approach could be extended and improved. For example, replicability scores could be used to test if the datasets considered have the same distribution, e.g. via permutation tests, or if specific clusters in the data are identical across datasets. We also imagine that versions of the cross-study metrics, with different data-points receiving different weights or upfront subsampling of the datasets, could be useful when the sizes of the datasets or clusters are highly imbalanced.

Acknowledgments

This work was partially supported by the National Science Foundation grant 1810829.

References

A. N. Albatineh, M. Niewiadomska-Bugaj, and D. Mihalko. On similarity indices and correction for chance agreement. *Journal of Classification*, 23(2), 2006.

G. Alexe, G. S. Dalgin, R. Ramaswamy, C. DeLisi, and G. Bhanot. Data perturbation independent diagnosis and validation of breast cancer subtypes using clustering and patterns. *Cancer Informatics*, 2, 2006.

S. Ben-David, D. Pál, and H. U. Simon. Stability of k -means clustering. In *International Conference on Computational Learning Theory*. Springer, 2007.

C. Bernau, M. Riester, A.-L. Boulesteix, G. Parmigiani, C. Huttenhower, L. Waldron, and L. Trippa. Cross-study validation for the assessment of prediction algorithms. *Bioinformatics*, 30(12), 2014.

A. Bertoni and G. Valentini. Model order selection for bio-molecular data clustering. *BMC Bioinformatics*, 8(2), 2007.

G. Brock, V. Pihur, S. Datta, and S. Datta. clvalid: An R package for cluster validation. *Journal of Statistical Software*, 25, 2008.

J. Bryan. Problems in gene clustering based on gene expression data. *Journal of Multivariate Analysis*, 90(1), 2004.

S. Dudoit and J. Fridlyand. A prediction-based resampling method for estimating the number of clusters in a dataset. *Genome Biology*, 3(7), 2002.

M. Ester, H.-P. Kriegel, J. Sander, and X. Xu. A density-based algorithm for discovering clusters in large spatial databases with noise. *Proceedings of the Second International Conference on Knowledge Discovery and Data Mining*, 1996.

Y. Fang and J. Wang. Selection of the number of clusters via the bootstrap method. *Computational Statistics & Data Analysis*, 56(3), 2012.

P. Fränti and S. Sieranoja. K-means properties on six clustering benchmark datasets. *Applied Intelligence*, 48(12), 2018.

P. Fränti, O. Virmajoki, and V. Hautamäki. Fast agglomerative clustering using a k -nearest neighbor graph. *IEEE Transactions on Pattern Analysis and Machine Intelligence*, 28(11), 2006.

B. J. Frey and D. Dueck. Clustering by passing messages between data points. *Science*, 315(5814), 2007.

B. Haibe-Kains, C. Desmedt, S. Loi, A. C. Culhane, G. Bontempi, J. Quackenbush, and C. Sotiriou. A three-gene model to robustly identify breast cancer molecular subtypes. *Journal of the National Cancer Institute*, 104(4), 2012.

D. N. Hayes, S. Monti, G. Parmigiani, C. B. Gilks, K. Naoki, A. Bhattacharjee, M. A. Socinski, C. Perou, and M. Meyerson. Gene expression profiling reveals reproducible human lung adenocarcinoma subtypes in multiple independent patient cohorts. *Journal of Clinical Oncology*, 24(31), 2006.

C. Hennig. Cluster-wise assessment of cluster stability. *Computational Statistics & Data Analysis*, 52(1), 2007.

C. Hennig. Package ‘fpc’. Available at: Available at: <https://cran.r-project.org/web/packages/fpc/index.html>, 91, 2015.

L. Hubert and P. Arabie. Comparing partitions. *Journal of Classification*, 2(1), 1985.

P. A. Jaskowiak, R. J. Campello, and I. G. Costa. On the selection of appropriate distances for gene expression data clustering. *BMC Bioinformatics*, 15(2):S2, 2014.

A. V. Kapp and R. Tibshirani. Are clusters found in one dataset present in another dataset? *Biostatistics*, 8(1), 2006.

H. O. Lancaster and E. Seneta. Chi-square distribution. *Encyclopedia of Biostatistics*, 2, 1969.

T. Lange, V. Roth, M. L. Braun, and J. M. Buhmann. Stability-based validation of clustering solutions. *Neural Computation*, 16(6), 2004.

P. Langfelder, R. Luo, M. C. Oldham, and S. Horvath. Is my network module preserved and reproducible? *PLoS Computational Biology*, 7(1), 2011.

M. A. Levenstien, Y. Yang, and J. Ott. Statistical significance for hierarchical clustering in genetic association and microarray expression studies. *BMC Bioinformatics*, 4(1), 2003.

E. Levine and E. Domany. Resampling method for unsupervised estimation of cluster validity. *Neural Computation*, 13(11), 2001.

Y. Liu, D. N. Hayes, A. Nobel, and J. S. Marron. Statistical significance of clustering for high-dimension, low-sample size data. *Journal of the American Statistical Association*, 103(483), 2008.

S. Lloyd. Least squares quantization in PCM. *IEEE Transactions on Information Theory*, 28(2), 1982.

L. v. d. Maaten and G. Hinton. Visualizing data using t-SNE. *Journal of Machine Learning Research*, 9(Nov), 2008.

L. M. McShane, M. D. Radmacher, B. Freidlin, R. Yu, M.-C. Li, and R. Simon. Methods for assessing reproducibility of clustering patterns observed in analyses of microarray data. *Bioinformatics*, 18(11), 2002.

N. A. of Sciences Engineering and Medicine. *Reproducibility and replicability in science*. National Academies Press, 2019.

J. S. Parker, M. Mullins, M. C. Cheang, S. Leung, D. Voduc, T. Vickery, S. Davies, C. Fauron, X. He, Z. Hu, J. F. Quackenbush, I. J. Stijleman, J. Palazzo, J. Marron, A. B. Nobel, E. Mardis, T. O. Nielsen, M. J. Ellis, C. M. Perou, and P. S. Bernard. Supervised risk predictor of breast cancer based on intrinsic subtypes. *Journal of Clinical Oncology*, 27(8), 2009.

C. M. Perou, T. Sørlie, M. B. Eisen, M. Van De Rijn, S. S. Jeffrey, C. A. Rees, J. R. Pollack, D. T. Ross, H. Johnsen, L. A. Akslen, et al. Molecular portraits of human breast tumours. *Nature*, 406(6797), 2000.

W. M. Rand. Objective criteria for the evaluation of clustering methods. *Journal of the American Statistical Association*, 66(336), 1971.

M. Schroeder, B. Haibe-Kains, A. Culhane, C. Sotiriou, G. Bontempi, and J. Quackenbush. *breastCancerMAINZ: Gene expression dataset published by Schmidt et al. [2008] (MAINZ)*., 2011a. R package version 1.16.0.

M. Schroeder, B. Haibe-Kains, A. Culhane, C. Sotiriou, G. Bontempi, and J. Quackenbush. *breastCancerTRANSBIG: Gene expression dataset published by Desmedt et al. [2007] (TRANSBIG)*., 2011b. R package version 1.16.0.

M. Schroeder, B. Haibe-Kains, A. Culhane, C. Sotiriou, G. Bontempi, and J. Quackenbush. *breastCancerVDX: Gene expression datasets published by Wang et al. [2005] and Minn et al. [2007] (VDX)*, 2011c. R package version 1.16.0.

M. Smolkin and D. Ghosh. Cluster stability scores for microarray data in cancer studies. *BMC Bioinformatics*, 4(1), 2003.

R. Tibshirani and G. Walther. Cluster validation by prediction strength. *Journal of Computational and Graphical Statistics*, 14(3), 2005.

L. Trippa, L. Waldron, C. Huttenhower, G. Parmigiani, et al. Bayesian nonparametric cross-study validation of prediction methods. *The Annals of Applied Statistics*, 9(1), 2015.

N. X. Vinh and J. Epps. A novel approach for automatic number of clusters detection in microarray data based on consensus clustering. In *2009 Ninth IEEE International Conference on Bioinformatics and BioEngineering*, 2009.

N. X. Vinh, J. Epps, and J. Bailey. Information theoretic measures for clusterings comparison: is a correction for chance necessary? In *Proceedings of the 26th Annual International Conference on Machine Learning*. ACM, 2009.

N. X. Vinh, J. Epps, and J. Bailey. Information theoretic measures for clusterings comparison: Variants, properties, normalization and correction for chance. *Journal of Machine Learning Research*, 11(Oct), 2010.

U. Von Luxburg et al. Clustering stability: an overview. *Foundations and Trends in Machine Learning*, 2(3), 2010.

A. G. Waks and E. P. Winer. Breast cancer treatment: A review. *JAMA*, 321(3), 2019.

J. H. Ward Jr. Hierarchical grouping to optimize an objective function. *Journal of the American Statistical Association*, 58(301), 1963.

T. Zhang, R. Ramakrishnan, and M. Livny. Birch: an efficient data clustering method for very large databases. In *ACM Sigmod Record*. ACM, 1996.

A Additional experiments on synthetic data

A.1 Calibration checks for the bootstrap intervals: experimental setup

To assess the quality of the bootstrap intervals that are obtained as a byproduct of the output of Algorithm 1 in the main text, we perform the following procedure. Let F_1 and F_2 be two fixed probability distributions with support on \mathbb{R}^p . Let \mathcal{A} be a fixed clustering algorithm.

Draw n i.i.d. random replicates x_1, \dots, x_n from F_1 , and let $\mathbf{X} = [x_1, \dots, x_n]^\top \in \mathbb{R}^{n \times p}$ be the training set. Similarly, draw m i.i.d. random replicates x'_1, \dots, x'_n from F_2 , and let $\mathbf{X}' = [x'_1, \dots, x'_m]^\top \in \mathbb{R}^{m \times p}$ be the testing dataset. Run Algorithm 1, as detailed in the main text, over a large number B of bootstrap draws from \mathbf{X} and \mathbf{X}' respectively. Given the output $\hat{R}^{(1)}, \dots, \hat{R}^{(B)}$, and for a fixed $\alpha \in [0, 1]$, let $\hat{R}_{(\alpha)}$ be the $100 \times \alpha\%$ quantile of the bootstrap scores $\hat{R}^{(1)}, \dots, \hat{R}^{(B)}$.

To assess the quality of the bootstrap intervals obtained from $\hat{R}_{(\alpha)}$, we compare them to corresponding Monte Carlo values, obtained by repeatedly drawing from F_1 and F_2 . In detail, fix a large N_{MC} . For each $s = 1, \dots, N_{MC}$, draw n i.i.d. random replicates $z_1^{(s)}, \dots, z_n^{(s)}$ from F_1 , and n i.i.d. random replicates $z_1^{(s)}, \dots, z_n^{(s)}$ from F_2 ; let $\mathbf{Z}^{(s)} = [z_1^{(s)}, \dots, z_n^{(s)}]^\top$ and $\mathbf{Z}'^{(s)} = [z_1'^{(s)}, \dots, z_n'^{(s)}]^\top$. Compute the replicability score $\hat{R}^{(s)} := r^*(\Psi(\mathbf{Z}'^{(s)}; \mathcal{A}, \mathbf{Z}^{(s)}), \Psi(\mathbf{Z}'^{(s)}; \mathcal{A}, \mathbf{Z}'^{(s)}))$. Given the output $\hat{R}^{(1)}, \dots, \hat{R}^{(N_{MC})}$, and for a fixed $\alpha \in [0, 1]$, let $\hat{R}_{(\alpha)}$ be the $100 \times \alpha\%$ quantile of the Monte Carlo scores $\hat{R}^{(1)}, \dots, \hat{R}^{(N_{MC})}$.

Experimental details

We present experimental results for the setup described above. Here, we let $n = m = 500$, $p = 2$, $B = 1000$, and $N_{MC} = 1000$. The algorithm \mathcal{A} is k -means. We also let F_1 , F_2 be mixtures of Gaussians, of the form:

$$F_1 = \frac{1}{4} \sum_{j=1}^4 \mathcal{N}(\mu_j, \sigma I), \quad F_2 = \frac{1}{4} \sum_{j=1}^4 \mathcal{N}(\mu'_j, \sigma I),$$

with $\sigma = 1$, and $\mu_1 = [0, -7], \mu_2 = [3.5, 3], \mu_3 = [-2, 2], \mu_4 = [2, -2]$ and $\mu'_1 = [-1, -7], \mu'_2 = [4.2, 3.3], \mu'_3 = [-2.5, 1.8], \mu'_4 = [2.2, -3]$.

We compare the average replicability score over the Monte Carlo and the bootstrap replicates, together with a centered 95% interval, as we vary the choice k of the number of clusters in Figure 7. We find that, across k , the bootstrap and Monte Carlo values are very close, showing that the bootstrap intervals enjoy good calibration.

Next, we inspect in Figure 8 the calibration of the bootstrap quantiles with respect to the Monte Carlo quantiles. That is, for each α in $[0, 1]$, we compare

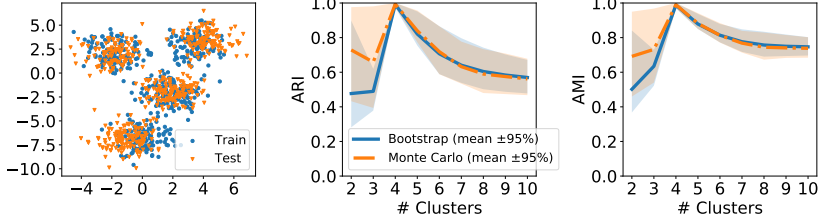


Figure 7: Left: draws $\mathbf{X} \in \mathbb{R}^{500,2}$ (blue), $\mathbf{X}' \in \mathbb{R}^{500,2}$ (orange) from train and test distributions F_1 and F_2 respectively. Center: ARI replicability score when using k -means (vertical axis) for different choices of k (horizontal axis). The blue line reports the average score over $B = 1000$ bootstrap replicates for the two datasets plotted in the left subplot. The orange dotted line reports the average score over $N_{MC} = 1000$ Monte Carlo draws of different pairs of training and testing datasets, drawn the same distributions F_1, F_2 above. Shadowed regions cover a centered 95% interval for the two scores.

the values $\hat{R}_{(\alpha)}$ and $\hat{\hat{R}}_{(\alpha)}$. We perform this comparison across different values of k , and verify that the bootstrap and Monte Carlo quantiles are close.

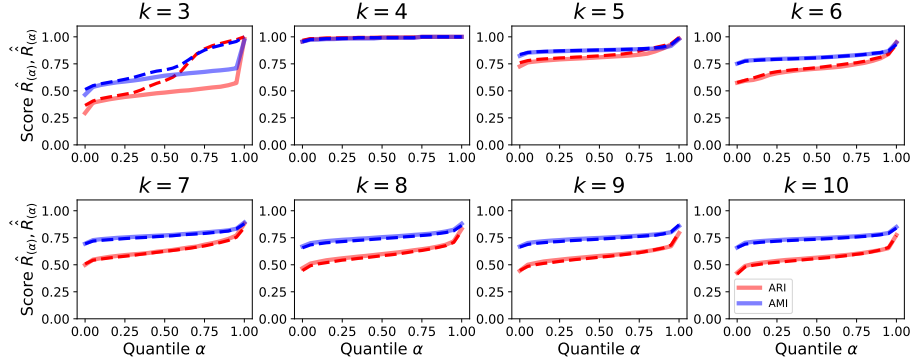


Figure 8: Quantiles coverage. For the same distributions F_1, F_2 considered in Figure 7, each subplot reports the bootstrap (solid lines, $\hat{R}_{(\alpha)}$) and Monte Carlo (dotted lines, $\hat{\hat{R}}_{(\alpha)}$) score (vertical axis) obtained as we increase the quantile (horizontal axis). Red lines refer to ARI, blue lines to AMI.

We repeat the same experiments, for different choices of F_1 and F_2 , ad defined below:

$$F_1 = \frac{1}{4} \sum_{j=1}^4 \mathcal{N}(\mu_j, \sigma I), \quad F_2 = \frac{1}{4} \sum_{j=1}^4 \mathcal{N}(\mu'_j, \sigma I),$$

now with $\mu_1 = [0, -7], \mu_2 = [3.5, -2], \mu_3 = [2, -2]$, and $\mu'_1 = [-1, -7], \mu'_2 = [4.2, -1.8], \mu'_3 = [-2.5, 1.8]$. Plots are included in Figures 9 and 10.

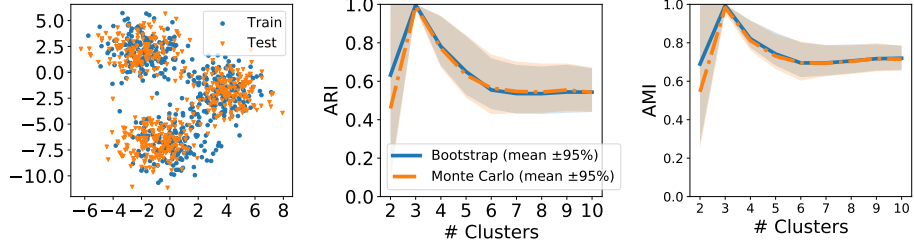


Figure 9: See Figure 7.

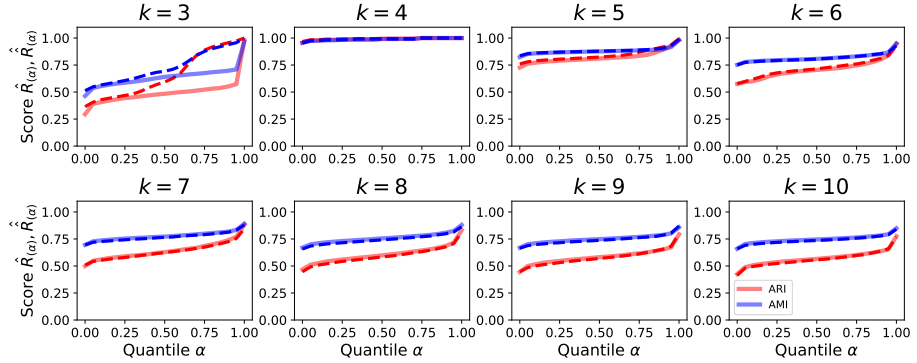


Figure 10: See Figure 8.

A.2 Replicability scores in the absence of clustering structure

To test whether our replicability metric is robust to the absence of clustering structure, we perform the following experiment. For fixed n , we draw $2n$ i.i.d. replicates x_1, \dots, x_{2n} from a fixed distribution F . We let $\mathbf{X} = [x_1, \dots, x_n]^\top$ and $\mathbf{X}' = [x_{n+1}, \dots, x_{2n}]^\top$ be the training and testing set respectively, and apply Algorithm 1 to inspect the behavior of the replicability scores on this data.

In our experiments below, we let F be the multivariate “standard” Gaussian, with mean the zero vector and covariance matrix the identity. In Figure 11 we fix $d = 2$ and vary $n \in \{200, 350, 500\}$. The qualitative finding from both the ARI and AMI scores are reassuring: in both cases the scores are low, and uniform across different choices of k .

Next, we inspect the behavior of the replicability scores across different choices of the dimension d of the random vectors drawn — $d \in \{5, 10, 15\}$, to understand the role of dimensionality. Again, scores are low, and uniform across different choices of k . Here $n = 200$.

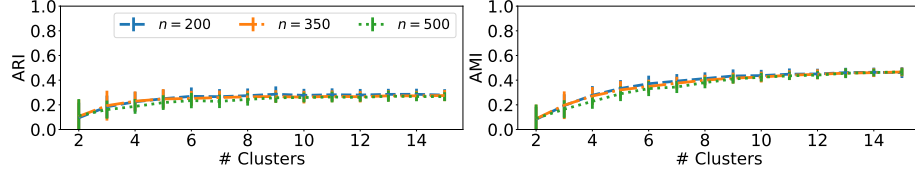


Figure 11: Replicability scores in the absence of clustering structure. We report the average replicability score \pm one standard deviation as obtained by $B = 100$ replicates according to Algorithm 1 (vertical axis, left: ARI, right: AMI) as we vary the number of clusters using k -means. Different line colors and styles refer to couples of training, testing datasets with different sizes n . Datapoints in the train and test dataset are i.i.d. multivariate Gaussian random draws with mean 0 and identity covariance matrix in \mathbb{R}^2 .

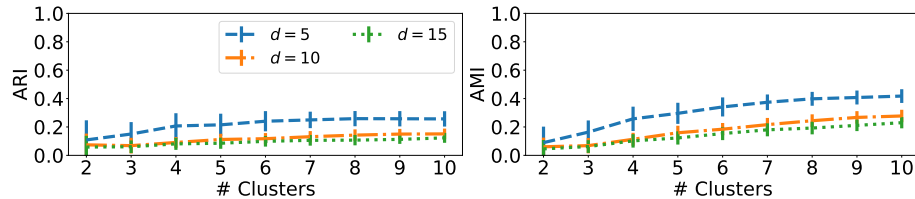


Figure 12: Replicability scores in the absence of clustering structure. We report the average replicability score \pm one standard deviation as obtained by $B = 100$ replicates according to Algorithm 1 (vertical axis, left: ARI, right: AMI) as we vary the number of clusters using k -means. Different line colors and styles refer to couples of training, testing datasets with different sizes n . Datapoints in the train and test dataset are i.i.d. multivariate Gaussian random draws with mean 0 and identity covariance matrix in \mathbb{R}^2 .

	Mainz	Transbig	Vdx
$ARI(\Pi_{PAM50}(\mathbf{X}), \Pi_{3G}(\mathbf{X}))$	0.33	0.34	0.53
$AMI(\Pi_{PAM50}(\mathbf{X}), \Pi_{3G}(\mathbf{X}))$	0.38	0.39	0.49

Table 1: Comparison of the subtype signatures for Mainz, Transbig and Vdx using either the three genes subset, or the PAM50 subset. For example, for the Mainz dataset, letting $\Pi_{PAM50}(\mathbf{mainz})$ and $\Pi_{3G}(\mathbf{mainz})$ be the PAM50 and 3G signatures (i.e. row-wise partitions) of the Mainz dataset, we compute $ARI(\Pi_{PAM50}(\mathbf{mainz}), \Pi_{3G}(\mathbf{mainz})) = 0.33$ and $AMI(\Pi_{PAM50}(\mathbf{mainz}), \Pi_{3G}(\mathbf{mainz})) = 0.38$.

B Additional figures and information about model-based signatures

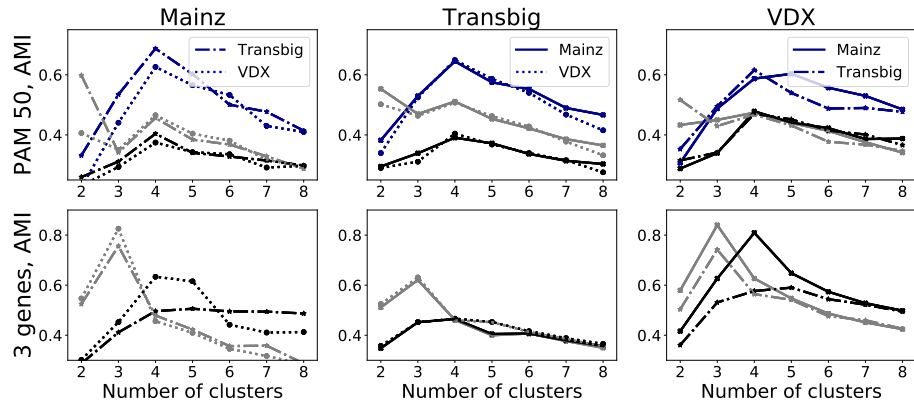


Figure 13: Each row refers to a different subset of genes (top row: PAM50 of Parker et al. [2009], bottom row: 3G of Haibe-Kains et al. [2012]). Each column refers to a different testing dataset \mathbf{X}' (left: Mainz, center: Transbig, right: VDX). For each gene subset, given testing dataset \mathbf{X}' , training dataset \mathbf{X} , algorithm \mathcal{A} and number of clusters k , we retain the partition $\Psi_{\mathbf{X}}^*(\mathbf{X}')$ and compare it to known signatures $\Pi_{PAM50}(\mathbf{X}')$ (top row) and $\Pi_{3G}(\mathbf{X}')$ (bottom row) by computing $AMI(\Psi_{\mathbf{X}}^*(\mathbf{X}'), \Pi_{PAM50}(\mathbf{X}'))$ (top row – y -axis) and $AMI(\Psi_{\mathbf{X}}^*(\mathbf{X}'), \Pi_{3G}(\mathbf{X}'))$ (bottom row – y -axis).